Accepted Manuscript

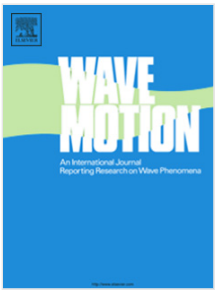

Wave propagation in two-dimensional anisotropic acoustic metamaterials of K4 topology

A.S. Fallah, Y. Yang, R. Ward, M. Tootkaboni, R. Brambleby, A. Louhghalam, L.A. Louca

PII: S0165-2125(15)00094-3
DOI: http://dx.doi.org/10.1016/j.wavemoti.2015.07.001
Reference: WAMOT 1961

To appear in: *Wave Motion*

Received date: 22 January 2013
Revised date: 29 June 2015
Accepted date: 1 July 2015

Please cite this article as: A.S. Fallah, Y. Yang, R. Ward, M. Tootkaboni, R. Brambleby, A. Louhghalam, L.A. Louca, Wave propagation in two-dimensional anisotropic acoustic metamaterials of K4 topology, *Wave Motion* (2015), http://dx.doi.org/10.1016/j.wavemoti.2015.07.001

Highlights

- Certain frequencies are filtered in metamaterials made of locally resonant units.
- Proportional anisotropy, K4 topology and attenuation-free plane waves are considered.
- Floquet-Bloch's principle is applied to irreducible Brillouin zone in **k**-space.
- Parametric studies show the direction and degree of influence of each variable.
- By tailoring mass, stiffness or aspect ratio desired frequencies are filtered.

Wave propagation in two-dimensional anisotropic acoustic metamaterials of K4 topology

A. S. Fallah[a*], Y. Yang[b], R. Ward[c], M. Tootkaboni[d], R. Brambleby[b], A. Louhghalam[e], L. A. Louca[b]

[a] *Centre for Nuclear Engineering, Department of Materials, Bessemer Building, South Kensington Campus, Imperial College London, SW7 2AZ, UK*

[b] *Department of Civil and Environmental Engineering, Skempton Building, South Kensington Campus, Imperial College London, SW7 2AZ, UK*

[c] *Department of Physics, Blackett Building, South Kensington Campus, Imperial College London, SW7 2AZ, UK*

[d] *Department of Civil and Environmental Engineering, University of Massachusetts Dartmouth, Dartmouth, MA 02747, USA*

[e] *Department of Civil and Environmental Engineering, Massachusetts Institute of Technology, 77 Massachusetts Avenue, Cambridge, MA 02139, USA*

Abstract

An acoustic metamaterial is envisaged as a synthesised phononic material the mechanical behaviour of which is determined by its unit cell. The present study investigates one aspect of mechanical behaviour, namely the band structure, in two-dimensional (2D) anisotropic acoustic metamaterials encompassing locally resonant mass-in-mass units connected by massless springs in a K4 topology. The 2D lattice problem is formulated in the direct space (**r**-space) and the equations of motion are derived using the principle of least action (Hamilton's principle). Only proportional anisotropy and attenuation-free shock wave propagation have been considered. Floquet-Bloch's principle is applied, therefore a generic unit cell is studied. The unit cell can represent the entire lattice regardless of its position. It is transformed from the direct lattice in **r**-space onto its reciprocal lattice conjugate in Fourier space (**k**-space) and point symmetry operations are applied to Wigner-Seitz primitive cell to derive the first irreducible Brillouin Zone (BZ). The edges of the first irreducible Brillouin Zone in the **k**-space have then been traversed to generate the full band structure. It was found that the phenomenon of frequency filtering exists and the pass and stop bands are extracted. A follow-up parametric study appreciated the degree and direction of influence of each parameter on the band structure.

Keywords:

[*] To whom correspondence should be addressed:
Tel: +44 (0) 2075946028
Fax: +44 (0) 2072252716
Email: arash.soleiman-fallah@imperial.ac.uk

Acoustic metamaterial, Band structure, Direct space (**r**-space), Fourier space (**k**-space), Floquet-Bloch's principle, Brillouin Zone (BZ), K4 topology

1. Introduction

An acoustic metamaterial is a member of the class known as phononic or mechphononic metamaterials. A phononic metamaterial is generally regarded as a material with an artificial microstructure which offers certain beneficial effects when wave propagation is relevant. Unlike natural materials, the mechanical behaviour of an acoustic metamaterial is not determined by its atomic microstructure but by its unit cell. Ubiquitous in the realm of electromagnetism (see e.g. [1-4]), metamaterials have started to receive attention in the fields of acoustics and applied mechanics [5-10]. Acoustic and phononic metamaterials have been the subject of some contemporary research due to the properties which distinguish them from natural materials. One such property, particularly of interest in acoustic applications, is the possibility to achieve negative mass density and elastic modulus [6, 10, 11] simultaneously in the strict sense of the effective medium theory [12]. This is similar to the negative refractive index in photonic metamaterials [2, 12]. The existence of a phononic/photonic band gap, i.e. an interval of frequencies over which mechanical/electromagnetic waves cannot propagate, is a direct consequence of this property and is of interest to engineers designing phononic/photonic devices[†]. Practical applications of such phononic devices include mechanical filters, vibration isolators, and acoustic waveguides [13, 14].

Many works of research have been conducted on phononic frequency pass and stop bands. To mention but a few, Kushwaha et al. [14] provided one of the earliest calculations of acoustic band gaps in a simple periodic composite. Nevertheless, their calculation was limited to the case of anti-plane shear. Zalipaev et al. [15] also considered anti-plane shear and studied the transition from two-dimensional (2D) wave propagation through the square periodic structure in time-harmonic case to a discrete parameter model of a 2D lattice with masses connected by springs. Martinsson [16] provided a simple method to calculate band gaps with special attention paid to the connection between microstructural geometry and the presence of band gaps. Lumped-mass method for the study of band structure in 2D phononic crystals was considered by Wang et al. [17]. They presented a lumped-mass model, based on the discretization of a continuous system, which works in the direct space (**r**-space) and allows computing the band structures of 2D phononic crystals. Li and Chan [11] studied doubly negative acoustic metamaterials in which both the effective density and bulk modulus are negative. Their double-negative acoustic system is an acoustic analogue of Veselago's medium in electromagnetism [18], and shares with it many

[†] The phenomenon of filtering in phononic devices could also be due to Bragg diffraction. The study of such cases falls beyond the scope of the present study.

principal features, such as negative refractive index, as a consequence of its microstructural composition. This implies the well-known analogy between mechanical and electrical systems known for almost two centuries [19]. Huang and Sun [20] studied the wave attenuation mechanisms in acoustic metamaterials of negative effective mass density. The metamaterial under consideration consists of locally resonant mass-in-mass units which, when homogenized, would have negative effective density. Any such homogenization theory allows for obtaining coarse-scale variation of field variables associated with a heterogeneous medium when the scale ratio, i.e. the ratio between fine and coarse scales, tends to zero while essential features are restored and represented faithfully. Locally resonant sonic materials were also studied by Liu et al. [8]. They fabricated sonic crystals, based on the idea of localized resonant structures, which exhibited spectral gaps with a lattice constant two orders of magnitude smaller than the relevant wavelength. Lattice constants refer to the directional distances between primitive/unit cells defined for a lattice material i.e. a material of reticulated structure obtained by tessellating the primitive cell along a finite number of fixed predefined directions.

Besides the studies conducted on wave propagation behaviour of lattices in the direct space (**r**-space), the reciprocal lattice formulation (formulation in **k**-space) is employed extensively by researchers. There are several advantages in employing the **k**-space formulation. To mention an example, in Truesdell continuum mechanics Helmholtz decomposition allows for lamellar and solenoidal parts of a vector field to be considered separately. The curl and divergence operators in **r**-space simply turn into cross and dot products in **k**-space, respectively. Kittel [21] and Brillouin [22] contain the details of the formulation of a wave problem in **k**-space. In a rather recent study, Phani et al. [23] investigated plane wave propagation in infinite 2D periodic lattices using Floquet-Bloch's principles. They formulated the exact finite element model of the problem based on the Timoshenko beam elements thus extracted frequency band gaps and examined spatial filtering phenomena in four representative planar lattice topologies viz. hexagonal honeycomb, Kagomé lattice, triangular honeycomb, and the square honeycomb. The plane-wave expansion method was used and the admissible plane wave solution was assumed attenuation-free which rendered Bloch's theorem applicable. This method was used by Yang et al. [24] to formulate the frequency filtering phenomenon in a heterogeneous metal-composite joint (a lattice problem) and using a plane stress super-element. They showed the band structure in a model of this sort and the benefit that filtering effects provide for such a system.

When an acoustic metamaterial is of the form of an infinite lattice with lumped masses and spring stiffness elements the band structure characteristics can be obtained using such a method. An interesting feature of such phononic metamaterials would then be the possibility to tailor the band structure by altering the inertial and stiffness properties of the primitive cell.

The objective of the present study is to investigate the band structure for anisotropic 2D acoustic metamaterials comprising locally resonant mass-in-mass units connected by spring stiffness elements in the simple topology of a complete graph on four vertices (K4)[‡]. The topology is selected in such a way that adequate redundancy requirement for quasi-static loading is also satisfied. Section 2 deals with the formulation of the representative anisotropic 2D acoustic metamaterial as an infinite lattice with lumped masses and discrete stiffness elements of different directional characteristics (thus the term "anisotropic"). The situation is similar to (but not exactly the same as) that of a locally resonant unit embedded in a matrix of a different material with vertical and horizontal distances of the units being different (source of anisotropy). In section 3 Floquet-Bloch's principle is applied to study the band structure of the 2D lattice. As the wave vector is assumed to be attenuation-free, the position of the primitive cell in the lattice is irrelevant to the change in the complex wave amplitude across the unit cell when a mechanical wave propagates in the lattice. The results obtained show the existence and the extent of the phenomenon of frequency filtering in this class of structures. This section is followed by section 4 which is a parametric study on mass and stiffness ratios. Only these ratios (rather than dimensional values) are important and physically meaningful. Thus, for the sake of the present study non-dimensional parameters are extracted and utilised using Buckingham's Pi-theorem. Only the case of "proportional" or "resembling" anisotropy is considered and the dependence of band structure on non-dimensional parameters observed is discussed. It has been shown that there is an optimal point at which the widest band gap of lower frequencies is achieved. The study is concluded in section 5.

2. The discrete parameter anisotropic 2D metamaterial

2.1. Formulation. Consider an infinite 2D medium comprising a countably infinite (of cardinality $\aleph_0$) number of locally resonant mass-in-mass units as shown in figure 1 placed periodically at distances *a* and *b* in directions *x* and *y*, respectively, and connected by axial springs in the topology of a complete graph on four vertices (K4) as depicted in figure 2a.The resulting metamaterial, shown in figure 2b, forms a repetitive structure i.e. a heterogeneous acoustic latticed system which forbids elastic wave propagation within its frequency band gap. If the model's material is linear elastic and geometric nonlinearity is disregarded the deformation of and interaction between the horizontal and vertical springs is assumed to have a negligible effect on the stiffness of springs i.e. the deformation of one spring does not affect the stiffness of either spring and the stiffness parameters of springs can be deduced independently and independent of the level of deformation. The stiffness and inertial

[‡] A complete graph on four vertices (K4) is obtained by placing four nodes (vertices or points) on a plane and connecting every pair of nodes by an edge (member or arc).

parameters of the mass-in-mass unit, along with the degrees of freedom, are shown in figure 1 and the geometric parameters are depicted in figure 2b where D is the diameter of the outer mass, a denotes the horizontal distance between the mass-in-mass units and b the vertical distance. The approximation in the calculations to be followed is based on the assumption that D is of a smaller order of magnitude compared to a and b i.e. $D/\min(a,b)<<1$. This renders both masses to be dealt with as particles (point masses) and rotatory inertia negligible. The length of the inclined spring is shown by $L=(a^2+b^2)^{1/2}$.

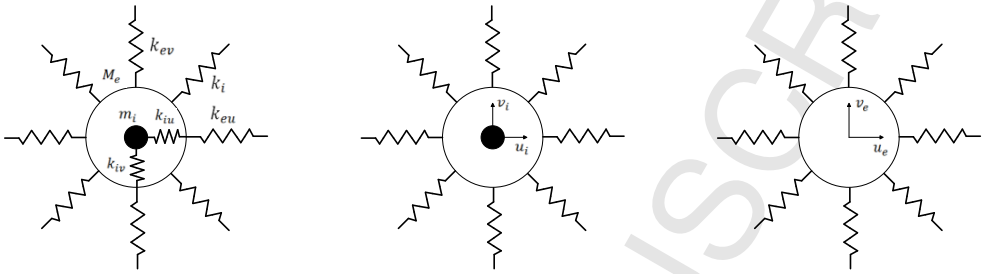

(a) (b) (c)

Figure 1: (a) Schematic of a locally resonant mass-in-mass unit (the building block of the anisotropic metamaterial) (b) the degrees of freedom of the internal mass particle (c) the degrees of freedom of the centre of mass of the external mass

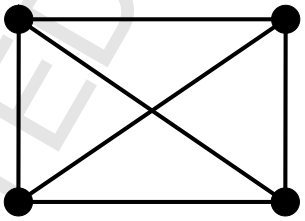

(a)

Figure 2: (a) the complete graph on four vertices (K4) (black circles denote the vertices (comprising both masses) and lines connecting them denote the edges), (b) the lumped mass-spring model of an acoustic metamaterial

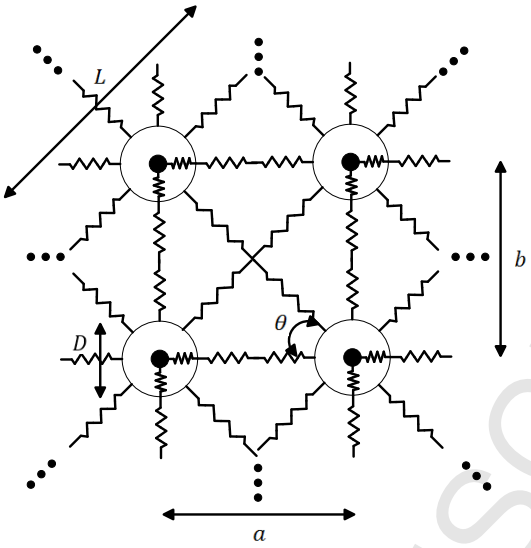

(b)

Figure 2: Cont'd

As mentioned before it is postulated that the rotatory inertia of outer masses is negligible thus each mass-in-mass unit can be regarded as two distinct particles interacting through the two internal springs only. There is further interaction between the outer masses of distinct units through outer springs. The connectivity of the 2D system requires each inner mass to be connected to the relevant outer mass through two springs in linearly independent (e.g. orthogonal) directions possessing not necessarily the same stiffness. The connectivity of units can be of several different forms but as stated before a simple K4 topology is assumed here. This can be regarded as a local (in contradistinction to nonlocal) interaction as the radius of interaction horizon is kept at minimum (L). The two internal orthogonal springs adopted here account for all possible interactions between the inner and outer masses.

A primitive cell of the lattice has been defined here the tessellating of which a units of length along horizontal (x) and b units of length along vertical (y) directions creates the entire metamaterial. Figure 3 shows a unit cell and its connectivity as well as the indices used for inner and outer masses of the unit cell at the p-th row and the q-th column of the lattice.

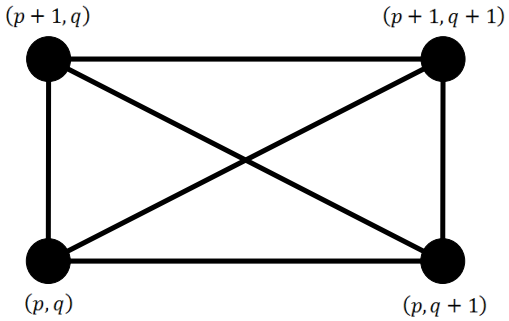

Figure 3: The unit cell and the superscript labels for degrees of freedom

As an assembly procedure is required to arrange the primitive cells into the lattice it must be noted that in the calculations of this study the masses in primitive cells are taken as quarter of the physical masses of the related mass-in-mass unit and the stiffness of the originally vertical and horizontal members in the primitive cell are half of those of the members in the lattice. It is evident that initially inclined members' stiffness is preserved. In the sequel we shall derive the equations of motion for a representative mass-in-mass unit using Lagrange's equations. We shall denote, as is customary, differentiation with respect to the time by an over-dot.

2.2. Equations of motion. The mass-in-mass unit placed on the *p*-th row and *q*-th column is labelled (*p*,*q*) (figure 3). The kinetic (*T*) and strain (*U*) energies which are additive integrals of the motion for a primitive cell of the acoustic metamaterial can be thus expressed by equations (1a)-(1f).

$$T = T_i + T_e \tag{1a}$$

$$T_i = \frac{1}{2}m_i\left(\dot{u}_i^{(p,q)^2} + \dot{v}_i^{(p,q)^2}\right) + \frac{1}{2}m_i\left(\dot{u}_i^{(p,q+1)^2} + \dot{v}_i^{(p,q+1)^2}\right) + \frac{1}{2}m_i\left(\dot{u}_i^{(p+1,q)^2} + \dot{v}_i^{(p+1,q)^2}\right) + \frac{1}{2}m_i\left(\dot{u}_i^{(p+1,q+1)^2} + \dot{v}_i^{(p+1,q+1)^2}\right) \tag{1b}$$

$$T_e = \frac{1}{2}m_e\left(\dot{u}_e^{(p,q)^2} + \dot{v}_e^{(p,q)^2}\right) + \frac{1}{2}m_e\left(\dot{u}_e^{(p,q+1)^2} + \dot{v}_e^{(p,q+1)^2}\right) + \frac{1}{2}m_e\left(\dot{u}_e^{(p+1,q)^2} + \dot{v}_e^{(p+1,q)^2}\right) + \frac{1}{2}m_e\left(\dot{u}_e^{(p+1,q+1)^2} + \dot{v}_e^{(p+1,q+1)^2}\right) \tag{1c}$$

$$U = U_i + U_e \tag{1d}$$

$$U_i = \frac{1}{2}k_{iu}(u_i^{(p,q)} - u_e^{(p,q)})^2 + \frac{1}{2}k_{iu}(u_i^{(p+1,q)} - u_e^{(p+1,q)})^2 + \frac{1}{2}k_{iu}(u_i^{(p,q+1)} - u_e^{(p,q+1)})^2 + \frac{1}{2}k_{iu}(u_i^{(p+1,q+1)} - u_e^{(p+1,q+1)})^2 + \frac{1}{2}k_{iv}(v_i^{(p,q)} - v_e^{(p,q)})^2 + \frac{1}{2}k_{iv}(v_i^{(p+1,q)} - v_e^{(p+1,q)})^2 + \frac{1}{2}k_{iv}(v_i^{(p,q+1)} - v_e^{(p,q+1)})^2 + \frac{1}{2}k_{iv}(v_i^{(p+1,q+1)} - v_e^{(p+1,q+1)})^2 \quad (1e)$$

$$U_e = \frac{1}{2}k_{eu}(u_e^{(p,q+1)} - u_e^{(p,q)})^2 + \frac{1}{2}k_{eu}(u_e^{(p+1,q+1)} - u_e^{(p+1,q)})^2 + \frac{1}{2}k_{ev}(v_e^{(p+1,q)} - v_e^{(p,q)})^2 + \frac{1}{2}k_{ev}(v_e^{(p+1,q+1)} - v_e^{(p,q+1)})^2 + \frac{1}{2}k_i(e_1^2 + e_2^2) \quad (1f),$$

Where e_1 and e_2 signify the elongation/contraction of the inclined members and are obtained as follows:

$$e_1 = u_e^{(p+1,q+1)}cos\theta - u_e^{(p,q)}cos\theta + v_e^{(p+1,q+1)}sin\theta - v_e^{(p,q)}sin\theta \quad (2a)$$

$$e_2 = u_e^{(p,q+1)}cos\theta - u_e^{(p+1,q)}cos\theta - v_e^{(p,q+1)}sin\theta + v_e^{(p+1,q)}sin\theta \quad (2b),$$

Where as shown in figures 1b and 1c the displacement components *u* and *v* lie in directions *x* and *y*, and the indices *i* and *e* refer to internal (inner) and external (outer) masses, respectively. The stiffness of the inclined elements is depicted by k_i. The governing ODE's for the primitive cell can now be obtained by using the principle of least action (Hamilton's principle) as follows:

$$\delta S = \delta \int_{t_1}^{t_2} L\mathrm{d}t = 0 \quad (3a)$$

$$L = T - U \quad (3b)$$

$$\frac{\partial L}{\partial w_i} = \frac{d}{dt}\left(\frac{\partial L}{\partial \dot{w}_i}\right) \quad (3c),$$

Where *S*, in equation (3a), is the action integral and *L* the Lagrangian of the system defined by equation (3b). Equation (3c) is an equation of motion for a generic degree of freedom and for cell arbitrarily placed in the lattice. w_i's are generalised coordinates which, in this case, are the same as physical components of the displacement vector due to the choice of the Cartesian coordinate system. It is obvious that due to this choice of co-ordinates kinetic energy is only a function of generalised velocities and strain energy only a function of generalised co-ordinates thus:

$$T = T_i + T_e = T\left(\dot{u}_i^{(m,n)}, \dot{u}_e^{(m,n)}, \dot{v}_i^{(m,n)}, \dot{v}_e^{(m,n)}\right) \qquad (4a)$$

$$U = U_i + U_e = U\left(u_i^{(m,n)}, u_e^{(m,n)}, v_i^{(m,n)}, v_e^{(m,n)}\right) \qquad (4b).$$

If a system of non-Cartesian generalised coordinates were adopted the form of strain energy would be preserved while the kinetic energy would be a function of generalised coordinates and generalised velocities. In any case the kinetic energy would be a quadratic function of generalised velocities. Using Lagrange's equations (3c) the equations of motion for the unit cell in position (*p*,*q*) are then derived as follows:

$$k_{iu}\left(u_i^{(p,q)} - u_e^{(p,q)}\right) + m_i\ddot{u}_i^{(p,q)} = 0 \qquad (5a)$$

$$k_{iu}\left(u_i^{(p+1,q)} - u_e^{(p+1,q)}\right) + m_i\ddot{u}_i^{(p+1,q)} = 0 \qquad (5b)$$

$$k_{iu}\left(u_i^{(p,q+1)} - u_e^{(p,q+1)}\right) + m_i\ddot{u}_i^{(p,q+1)} = 0 \qquad (5c)$$

$$k_{iu}\left(u_i^{(p+1,q+1)} - u_e^{(p+1,q+1)}\right) + m_i\ddot{u}_i^{(p+1,q+1)} = 0 \qquad (5d).$$

$$k_{iv}\left(v_i^{(p,q)} - v_e^{(p,q)}\right) + m_i\ddot{v}_i^{(p,q)} = 0 \qquad (6a)$$

$$k_{iv}\left(v_i^{(p+1,q)} - v_e^{(p+1,q)}\right) + m_i\ddot{v}_i^{(p+1,q)} = 0 \qquad (6b)$$

$$k_{iv}\left(v_i^{(p,q+1)} - v_e^{(p,q+1)}\right) + m_i\ddot{v}_i^{(p,q+1)} = 0 \qquad (6c)$$

$$k_{iv}\left(v_i^{(p+1,q+1)} - v_e^{(p+1,q+1)}\right) + m_i\ddot{v}_i^{(p+1,q+1)} = 0 \qquad (6d).$$

$$\begin{aligned} m_e^{(p,q)}\ddot{u}_e^{(p,q)} &- k_{iu}\left(u_i^{(p,q)} - u_e^{(p,q)}\right) - k_{eu}\left(u_e^{(p,q+1)} - u_e^{(p,q)}\right) \\ &- k_i\left(u_e^{(p+1,q+1)}cos\theta - u_e^{(p,q)}cos\theta + v_e^{(p+1,q+1)}sin\theta - v_e^{(p,q)}sin\theta\right)cos\theta \\ &= 0 \end{aligned} \qquad (7a)$$

$$\begin{aligned} m_e^{(p+1,q)}\ddot{u}_e^{(p+1,q)} &- k_{iu}\left(u_i^{(p+1,q)} - u_e^{(p+1,q)}\right) - k_{eu}\left(u_e^{(p+1,q+1)} - u_e^{(p+1,q)}\right) \\ &- k_i\left(u_e^{(p,q+1)}cos\theta - u_e^{(p+1,q)}cos\theta - v_e^{(p,q+1)}sin\theta + v_e^{(p+1,q)}sin\theta\right)cos\theta \\ &= 0 \end{aligned} \qquad (7b)$$

$$\begin{aligned} m_e^{(p,q+1)}\ddot{u}_e^{(p,q+1)} &- k_{iu}\left(u_i^{(p,q+1)} - u_e^{(p,q+1)}\right) + k_{eu}\left(u_e^{(p,q+1)} - u_e^{(p,q)}\right) \\ &+ k_i\left(u_e^{(p,q+1)}cos\theta - u_e^{(p+1,q)}cos\theta - v_e^{(p,q+1)}sin\theta + v_e^{(p+1,q)}sin\theta\right)cos\theta \\ &= 0 \end{aligned} \qquad (7c)$$

$$m_e^{(p+1,q+1)}\ddot{u}_e^{(p+1,q+1)} - k_{iu}\left(u_i^{(p+1,q+1)} - u_e^{(p+1,q+1)}\right) + k_{eu}\left(u_e^{(p+1,q+1)} - u_e^{(p+1,q)}\right) + k_i\left(u_e^{(p+1,q+1)}cos\theta - u_e^{(p,q)}cos\theta + v_e^{(p+1,q+1)}sin\theta - v_e^{(p,q)}sin\theta\right)cos\theta = 0 \quad (7d).$$

$$m_e^{(p,q)}\ddot{v}_e^{(p,q)} - k_{iv}\left(v_i^{(p,q)} - v_e^{(p,q)}\right) - k_{ev}\left(v_e^{(p+1,q)} - v_e^{(p,q)}\right) - k_i\left(u_e^{(p+1,q+1)}cos\theta - u_e^{(p,q)}cos\theta + v_e^{(p+1,q+1)}sin\theta - v_e^{(p,q)}sin\theta\right)sin\theta = 0 \quad (8a)$$

$$m_e^{(p+1,q)}\ddot{v}_e^{(p+1,q)} - k_{iv}\left(v_i^{(p+1,q)} - v_e^{(p+1,q)}\right) + k_{ev}\left(v_e^{(p+1,q)} - v_e^{(p,q)}\right) + k_i\left(u_e^{(p,q+1)}cos\theta - u_e^{(p+1,q)}cos\theta + v_e^{(p,q+1)}sin\theta - v_e^{(p+1,q)}sin\theta\right)sin\theta = 0 \quad (8b)$$

$$m_e^{(p,q+1)}\ddot{v}_e^{(p,q+1)} - k_{iv}\left(v_i^{(p,q+1)} - v_e^{(p,q+1)}\right) - k_{ev}\left(v_e^{(p+1,q+1)} - v_e^{(p,q+1)}\right) - k_i\left(u_e^{(p,q+1)}cos\theta - u_e^{(p+1,q)}cos\theta - v_e^{(p,q+1)}sin\theta + v_e^{(p+1,q)}sin\theta\right)sin\theta = 0 \quad (8c)$$

$$m_e^{(p+1,q+1)}\ddot{v}_e^{(p+1,q+1)} - k_{iv}\left(v_i^{(p+1,q+1)} - v_e^{(p+1,q+1)}\right) + k_{ev}\left(v_e^{(p+1,q+1)} - v_e^{(p,q+1)}\right) + k_i\left(u_e^{(p+1,q+1)}cos\theta - u_e^{(p,q)}cos\theta + v_e^{(p+1,q+1)}sin\theta - v_e^{(p,q)}sin\theta\right)sin\theta = 0 \quad (8d).$$

The 16 equations of motion above concern the unit cell and are arranged to reflect the horizontal (equations (5) and (7)) and vertical (equations (6) and (8)) motion of the internal (equations (5) and (6)) and external (equations (7) and (8)) masses. It will be shown that for harmonic wave propagation in the 2D resonator mass-in-mass latticed system formulated as above, waves of certain frequencies will not be able to pass through the medium, irrespective of their amplitude.

3. Frequency analysis

3.1. Floquet-Bloch's principle. This principle (also known as Bloch's theorem) renders possible the consideration of a single primitive or unit cell for studying wave propagation in the entire lattice structure. If the radius vectors of lattice points in a primitive cell are denoted by $\boldsymbol{r}_j$ and the arbitrary displacement component z of one such a point by $z(\boldsymbol{r}_j)$, then for a harmonic plane wave solution the displacement component is of the form:

$$z(\boldsymbol{r}_j) = Z_j e^{(i\omega t - \boldsymbol{k}.\boldsymbol{r})} \quad (9),$$

Where Z_j is the amplitude, ω is the frequency, t represents time and $\boldsymbol{k}$ represents the wave vector of the plane wave. Any other lattice point can be identified by vector summation of n_i translations in directions $\boldsymbol{e}_i$ of the associated point in the reference primitive cell (n_i being an integer). In the case of

a 2D lattice this will lead to the radius vector of an arbitrary point in the lattice being defined as follows:

$$\boldsymbol{r} = \boldsymbol{r}_j + n_i\boldsymbol{e}_i = \boldsymbol{r}_j + n_1\boldsymbol{e}_1 + n_2\boldsymbol{e}_2 \quad (10).$$

In the case of a plane wave the displacement at an arbitrary lattice point is obtained as follows with reference to a similarly placed point in the reference primitive cell:

$$z(\boldsymbol{r}) = z(\boldsymbol{r}_j)e^{\boldsymbol{k}.(\boldsymbol{r}-\boldsymbol{r}_j)} \quad (11).$$

The wave vector in general possesses complex components i.e. $k_j = \eta_j + i\varepsilon_j$ where the real part is called the "attenuation constant" and the imaginary part is termed the "phase constant" [21-23]. In simple terms Floquet-Bloch's principle states the fact that for a lattice structure the change in complex wave amplitude across a unit cell due to propagation of wave without attenuation (i.e. $\eta_j = 0$) is independent of the position of the unit cell. Hence, by studying wave propagation in a primitive cell the whole lattice will in fact be studied.

Another important concept is that of a Brillouin Zone (BZ). It is convenient to define a reciprocal lattice in the Fourier space (***k***-space) the bases of which satisfy the following condition of orthogonality:

$$\boldsymbol{e}_i^*.\boldsymbol{e}_j = \delta_{ij} \quad (12).$$

Where δ_{ij} is the second order identity tensor i.e. Kronecker's delta which also acts as a substitution operator. The first BZ [22] is then defined as a Wigner-Seitz primitive cell in the reciprocal lattice space [21] following a simple procedure as explained below:

(1) Select any lattice point in the reciprocal lattice and connect it to its immediately adjacent points using straight lines. A rectilinear isomorphic of a star graph is constructed with the initially chosen lattice point as the origin.

(2) Construct the normal bisectors of the straight segments (edges). The minimal region bounded inside the bisectors is a Wigner-Seitz primitive cell which for the reciprocal lattice signifies the first Brillouin Zone.

The first irreducible BZ is studied. Hence, the study of wave propagation in this region will provide the band structure for the whole lattice. A parameter *s* is defined to represent the arc length along the edges of the first irreducible BZ. It can be shown that the extraction of the band gap in the whole lattice will have been complete if wave vectors are restricted to the edges of this region [21]. Figure 4

depicts the ***k***-space locus which along with the coordinates of the points given in table 1 specifies the irreducible zone.

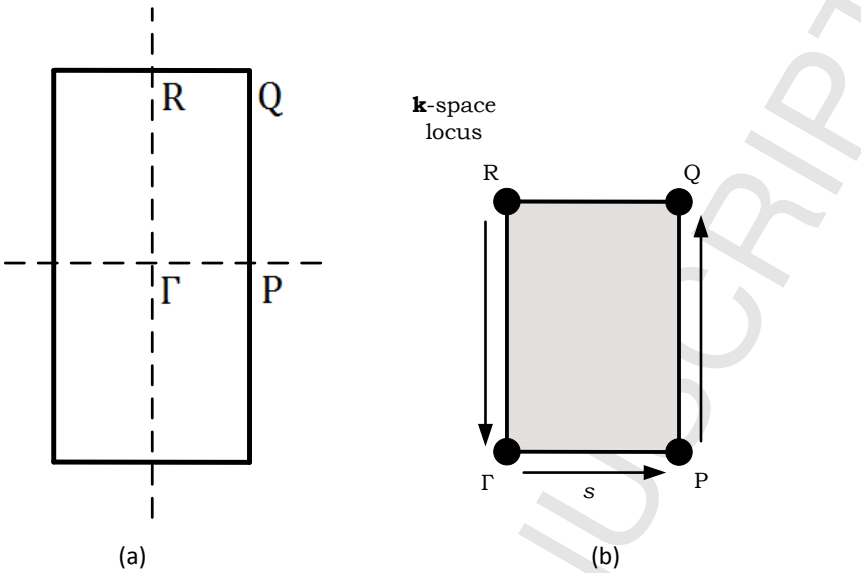

Figure 4: (a) the Brillouin Zone (BZ) (b) the irreducible first Brillouin Zone

Γ	P	Q	R
(0, 0)	(π/a, 0)	(π/a, π/b)	(0, π/b)

Table 1: The coordinates of points of the first irreducible zone (***k***-space)

3.2. Band structure. The equations of motion derived in the previous section are used to study the band structure in the lattice, the primitive cell of which is given in figure 3, and consequently possesses the irreducible BZ of figure 4. By applying Bloch's theorem to the first irreducible BZ in the ***k***-space, equation (9) can be rewritten as $\mathbf{u}_{\mathrm{nk}}(\mathbf{r}_{\mathrm{j}}+\mathbf{T}_{\mathrm{L}})=\mathbf{u}_{\mathrm{nk}}(\mathbf{r}_{\mathrm{j}})e^{\boldsymbol{k}.\mathbf{T}_{\mathrm{L}}}$ with *n* being the band index, and $\boldsymbol{T_L}$ a translation vector of the lattice in ***k***-space. The following relations among the ***k***-space displacements can be obtained:

$$\mathbf{u_2}=\mathbf{u_1}e^{\mathrm{k}_2},\ \mathbf{u_3}=\mathbf{u_1}e^{\mathrm{k}_1+\mathrm{k}_2},\ \mathbf{u_4}=\mathbf{u_1}e^{\mathrm{k}_1} \qquad (13a)$$

$$\mathbf{v_2}=\mathbf{v_1}e^{\mathrm{k}_2},\ \mathbf{v_3}=\mathbf{v_1}e^{\mathrm{k}_1+\mathrm{k}_2},\ \mathbf{v_4}=\mathbf{v_1}e^{\mathrm{k}_1} \qquad (13b),$$

Where $\boldsymbol{u}_n$ includes the horizontal components of the displacement vector for node *i* i.e. $\mathbf{u_n}=\begin{bmatrix}u_i^n\\u_e^n\end{bmatrix}$.

As an example the first equation in (13a) then represents: $\begin{bmatrix}u_i^2\\u_e^2\end{bmatrix}=\begin{bmatrix}u_i^1\\u_e^1\end{bmatrix}e^{k_2}$

$\boldsymbol{v}_i$ is defined in a similar manner. The translation vector is $\boldsymbol{T}_L$=$\mathbf{e_2}$ for point 2, $\boldsymbol{T}_L$= $\mathbf{e_1}$+$\mathbf{e_2}$ for point 3 and $\boldsymbol{T}_L$=$\mathbf{e_1}$ for point 4. Figure 5 depicts the dependent degrees of freedom which are associated with the nodes bounded in the dashed line. Equations (13) can be restated on a rearrangement of the degrees of freedom as equation (14) where the transformation matrix $\mathbf{T}_B$ is defined by equation (15) (as in [23]):

$$\mathbf{U_i} = \mathbf{T_B U_1} \qquad (14).$$

$$\mathbf{T}_B = \begin{bmatrix} \mathbf{I} & 0 & 0 & 0 \\ 0 & \mathbf{I} & 0 & 0 \\ \mathbf{I}e^{k_2} & 0 & 0 & 0 \\ 0 & \mathbf{I}e^{k_2} & 0 & 0 \\ \mathbf{I}e^{k_1+k_2} & 0 & 0 & 0 \\ 0 & \mathbf{I}e^{k_1+k_2} & 0 & 0 \\ \mathbf{I}e^{k_1} & 0 & 0 & 0 \\ 0 & \mathbf{I}e^{k_1} & 0 & 0 \\ 0 & 0 & \mathbf{I} & 0 \\ 0 & 0 & 0 & \mathbf{I} \\ 0 & 0 & \mathbf{I}e^{k_2} & 0 \\ 0 & 0 & 0 & \mathbf{I}e^{k_2} \\ 0 & 0 & \mathbf{I}e^{k_1+k_2} & 0 \\ 0 & 0 & 0 & \mathbf{I}e^{k_1+k_2} \\ 0 & 0 & \mathbf{I}e^{k_1} & 0 \\ 0 & 0 & 0 & \mathbf{I}e^{k_1} \end{bmatrix} \qquad (15),$$

with $\mathbf{U}_i = [u_i^1 \;\; v_i^1 \;\; u_i^2 \;\; v_i^2 \;\; u_i^3 \;\; v_i^3 \;\; u_i^4 \;\; v_i^4 \;\; u_e^1 \;\; v_e^1 \;\; u_e^2 \;\; v_e^2 \;\; u_e^3 \;\; v_e^3 \;\; u_e^4 \;\; v_e^4 \;]^T$ and $\mathbf{U}_1 = [u_i^1 \;\; v_i^1 \;\; u_e^1 \;\; v_e^1]^T$ and where $\boldsymbol{I}$ is the 1x1 identity matrix i.e. $\boldsymbol{I}$=1.The choice of this notation is preferable as a generalisation of the study to cases with more degrees of freedom or different topologies is rendered possible.

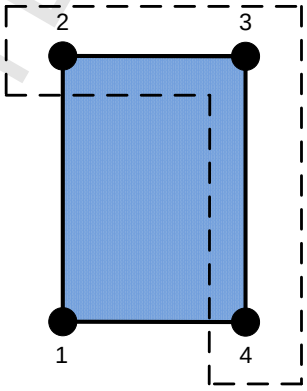

Figure 5: The nodes bounded by dashed lines represent the dependent degrees of freedom, node 1 degrees of freedom represnt Bloch reduced coordinates

For the free vibration of the lattice the equations of motion (equations (5)-(8)) take the following conventional form:

$$\boldsymbol{M\ddot{u} + Ku = 0} \quad (16).$$

By applying Bloch's theorem and considering plane wave solution of equation (9), equation (16) can be re-cast in the following form:

$$\boldsymbol{\tilde{D}u = 0} \quad (17),$$

Where $\boldsymbol{\tilde{D} = T_B^H D\, T_B}$ with $\boldsymbol{D}$ being the dynamic matrix defined as $\boldsymbol{D = K - M\omega^2}$ and the superscript *H* denoting Hermitian transposition. Equation (17) then defines an algebraic eigenvalue problem as follows:

$$\boldsymbol{\tilde{D}(k, \omega^2)u = \tilde{D}}(k_1, k_2, \omega^2)\boldsymbol{u = 0} \quad (18).$$

As it has been assumed that wave propagates with no attenuation in the 2D acoustic metamaterial, (i.e. $k_1 = i\varepsilon_1$ and $k_2 = i\varepsilon_2$), the associated eigenvalue problem only includes two components of the wave vector viz. the phase constants ε_1 and ε_2 which along with the frequency of the plane wave ω form the complete solution.

As discussed earlier, due to the periodicity, the phase constants ε_1 and ε_2 can be specified to restrict the wave vector to the edges of the irreducible part of the 1st Brillouin Zone. (i.e. $\boldsymbol{k} \in [-\pi, \pi]^d$, where *d* is the dimension of the space (here 2)). Any other point $\boldsymbol{k}$ of the zone which is not in this rectangle can be rotated into a $\boldsymbol{k}$-vector inside the rectangle by a symmetry operation that leaves the zone invariant. Based on these, dispersion surfaces can be computed by solving for the frequencies. The complete procedure for the derivation of the band diagrams as well as an example derivation is included in Appendix A. As a special case the 1D metamaterial of Huang and Sun [20] has been considered and its band diagrams have been extracted using the proposed method. These are then correlated with those obtained originally by Huang and Sun based on a different method. The two sets of results show the excellent correlation and confirm further the correctness of the results presented in this paper.

The results for some cases are presented and discussed in the next section.

4. Parametric studies

A set of non-dimensional parameters can be obtained based on the parameters defining the problem uniquely and by the application of Buckingham's Pi-theorem. Let the number of dimensional parameters defining the model be n and the rank of the dimensionality matrix r, then the cardinality of the set of dimensionless parameters is $n-r$. These parameters along with r dimensional ones define necessarily the same problem, uniquely. The following dimensionless parameters are extracted for the problem under consideration for which $n=8$ and $r=2$.

$$\pi_1 = \alpha = \frac{m_i}{M_e} \tag{19a}$$

$$\pi_2 = \beta = \frac{k_{iu}}{k_{eu}} \tag{19b}$$

$$\pi_3 = \frac{k_{iv}}{k_{ev}} \tag{19c}$$

$$\pi_4 = \frac{k_{eu}}{k_{ev}} \tag{19d}$$

$$\pi_5 = \frac{k_i}{k_{ev}} \tag{19e}$$

$$\pi_6 = \frac{k_{eu}}{M_e\omega^2} \tag{19f},$$

Where π_6 is the response parameter (output), and all other parameters are inputs. As brevity is intended only a special case of anisotropy termed "proportional anisotropy" or "resembling anisotropy" is considered which assumes $\pi_2 = \pi_3$. A total number of 27 models have been considered with the characteristics of each model being included in table 2 along with sizes of any full band gap. Where multiple band gaps were present, the sizes were ordered in this table from lower to higher frequencies. It may be more convenient, as well as geometrically more meaningful, to choose a different dimensionless parameter ($\gamma = a/b$) , instead of π_4 , for the sake of the parametric studies in this section. Similarly, in the special case of anisotropy considered $\pi_5 = (\gamma^2+1)^{-1}$. As mentioned previously, 3x3x3=27 models are considered for the sake of parametric studies of this section. Figure 6 depicts a typical frequency band diagram and explains what is meant by full and partial band gaps. While certain frequencies are filtered when wave vector is in particular direction for the case of a partial band gap, a full (complete) band gap filters out a range of frequencies irrespective of wave direction. The frequency intervals other than band gaps (stop bands) are known as pass bands. Figures

7(1)-7(3) (example cases 2, 15 and 25) show some of the results of the parametric studies conducted while Appendix B includes the results for all 27 models concerned. In each such diagram the abscissa shows the edge arc length parameter (s) introduced in figure 4 and the ordinate is the non-dimensional frequency normalised with respect to the natural frequency of the internal mass in the horizontal direction ($\hat{\omega}_i = {}^{\omega_i}/_{\omega_{ref}}$) as the reference frequency. The choice of this response parameter is physically more meaningful.

		α = 0.1	α = 1	α = 10
β = 0.1	γ = 0.50	Case 1, Gap = 0.000	Case 4, Gap = 0.002	Case 7, Gap = 0.216
	γ = 0.75	Case 2, Gap = 0.000	Case 5, Gap = 0.037	Case 8, Gap = 0.299
	γ = 1.00	Case 3, Gap = 0.009	Case 6, Gap = 0.067	Case 9, Gap = 0.370
β = 1	γ = 0.50	Case 10, Gaps = 0.017 & 0.036	Case 13, Gap = 0.017	Case 16, Gap = 0.229
	γ = 0.75	Case 11, Gaps = 0.034 & 0.011	Case 14, Gap = 0.050	Case 17, Gap = 0.310
	γ = 1.00	Case 12, Gap = 0.048	Case 15, Gap = 0.078	Case 18, Gap = 0.379
β = 10	γ = 0.50	Case 19, Gaps = 0.085 & 0.048	Case 22, Gaps = 0.087 & 0.044	Case 25, Gaps = 0.285 & 0.022
	γ = 0.75	Case 20, Gaps = 0.107 & 0.022	Case 23, Gaps = 0.116 & 0.008	Case 26, Gap = 0.363
	γ = 1.00	Case 21, Gap = 0.127	Case 24, Gap = 0.140	Case 27, Gap = 0.428

Table 2: Models specifications and band gap sizes

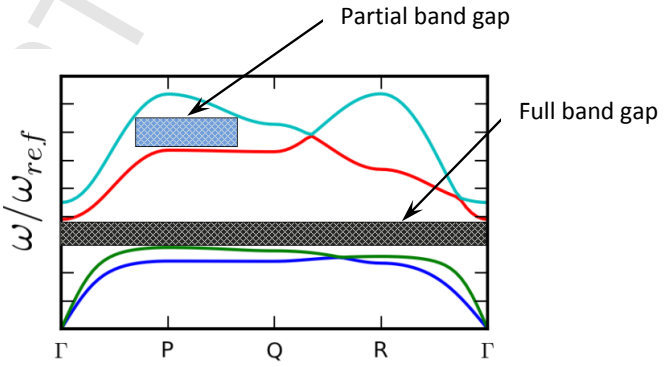

Figure 6: Band structure with Full band (forbidden) gap and Partial band gap

A comparison of each case (i) with cases (i+1) and (i+2), (i=3k+1, k=0,1,…) shows the effect of parameter (γ=a/b). As γ, the aspect ratio of the primitive cell, increases a wider range of lower frequencies are filtered out while higher frequency components of response are no longer absent. This shows the beneficial effect of anisotropy in filtering higher frequency components of the response provided wave direction is known *a priori*. These results are consistent and are observed in all cases irrespective of mass and stiffness ratios. The cases γ=1 i.e. i=3k correspond to isotropic 2D metamaterials. In this situation the first irreducible BZ turns into a right triangle the sides of which are half the sides and half the diagonal of the square. Due to resembling anisotropy this implies complete lattice isotropy. The band structure in any such case must be symmetric about point Q on the ***k***-space locus. This is observed in all such cases. In any case, the effect of this parameter on the band gap is less pronounced than that of the other two parameters involved i.e. α and β.

Comparison of each case (i) with cases (i+3) and (i+6), (i=3k+1, k=0,3,…) depicts the effect of mass ratio on band structure. Mass ratio (α), as defined by equation (19a), has a similar effect as aspect ratio i.e. by increasing this ratio; lower frequencies are filtered more efficiently while the situation is aggravated if filtering higher frequencies is of interest. The effect of mass ratio on wave propagation can be perceived as the similar case of a simple tune mass damper (TMD) (the electrical analogue of which is an LCR circuit). This ratio can be tuned to provide the desired band structure. A TMD can filter out one frequency and an infinite reticulated structure such as a lattice or a metamaterial can filter out a range of frequencies.

When case (i) is compared to cases (i+9) and (i+18), (i=3k+1, k=0,1,…) the effect of stiffness ratio on band structure is clarified. Stiffness ratio i.e. $\beta = \pi_2 = \pi_3$ plays a similar role as mass ratio in the sense that lower frequencies are more pronouncedly filtered out when this ratio increases, however; there is a difference here. As the stiffness ratio increases the frequency curves flatten which implies the wider range of frequency filtering for lower frequencies while preserving some higher frequency filtering. In the extreme case when $\beta >> 1$ the two masses are connected by a rigid link. This implies no local resonance and the metamaterial behaves as an ordinary 2D lattice. Dispersion curves for this case can apparently be regenerated ignoring that the two particles are distinct and with the total mass of the two being condensed in the centre of mass as a single particle and connected to each other by external springs.

The frequency band structures included can be looked into from other angles as well since dimensionless parameters can be rearranged. The degree and direction of influence of dimensionless parameters on band structure evidently allow for tailoring capabilities to be achieved for metamaterials comprising locally resonant mass-in-mass units. Furthermore; the anisotropy of the lattice adds a new dimension in the sense that an optimal point can always be found in the space of

alternatives for which an intermediate frequency is filtered. For harmonic and periodic pulses the meaning is obvious. The important task would thus be converting a transient pulse (in *t*-domain) to amplitude vs. frequency curve in Fourier space (ω-domain) and find out the damaging frequencies with highest amplitudes. Then tailoring the metamaterial would render these components impossible to propagate.

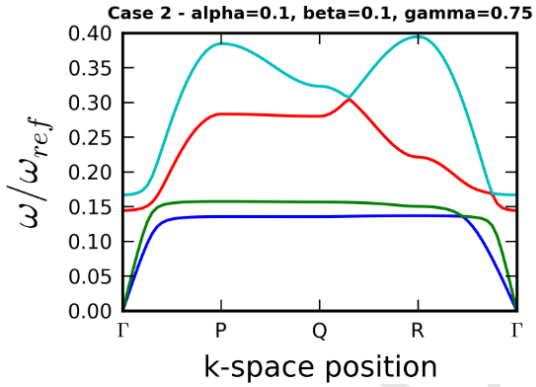

(a)

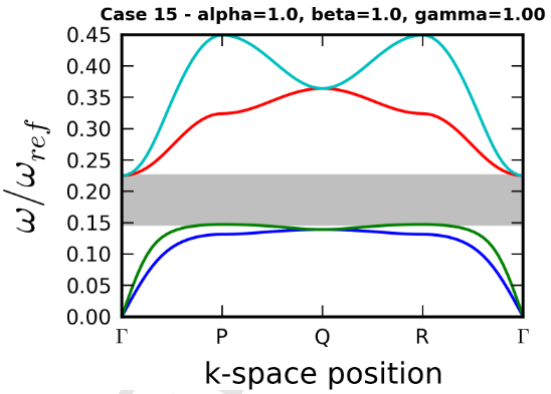

(b)

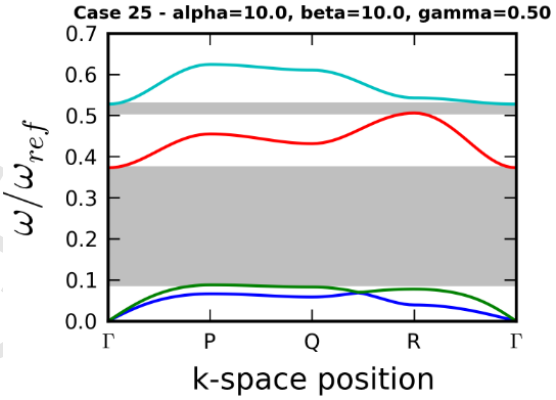

(c)

Figure 7: Band structure for three selected cases (2, 15 and 25)

The results above, as well as those of Appendix B, are auto-scaled to suit dispersion curves showing the dimensionless frequency normalised with respect to the local resonance frequency of internal mass.

5. Conclusions

The present study deals with extraction of band structure and the associated frequency filtering phenomenon in 2D anisotropic metamaterials composed of locally resonant mass-in-mass units connected by massless springs of a dissimilar material in a simple but from a redundancy viewpoint adequate topology i.e. the complete graph on four vertices (K4). The problem is formulated in the most general form and the equations of motion are derived by the application of Hamilton's principle. The metamaterial under consideration forms a direct lattice, a primitive cell of which is defined in ***r***-space. Although the formulation is general, due to relatively large number of parameters involved only a special case of anisotropy has been considered which is termed "proportional" or "resembling". Shock propagation without attenuation is assumed and Floquet-Bloch's principle is applied. When all point symmetry operations are taken into account the irreducible Brillouin zone of primitive cell's ***k***-space locus is obtained. The study of this zone suffices to extract band diagrams. The phenomenon of frequency filtering is observed and the band structure is extracted. A parametric study is conducted with 27 cases involved and the degree and direction of influence of each dimensionless parameter on the band structure is appreciated and expounded. It is shown that by tailoring the mass ratio, aspect ratio and stiffness ratio at a time both lower and higher frequencies can be filtered. The task would thus be to determine the damaging frequency contents of an external pulse load. As anisotropy introduces a new factor, the model proposed is more sophisticated and more capable of being tailored than its isotropic counterpart. Tuning can also be achieved by not restricting oneself to proportional anisotropy. One final remark regarding the dispersion curves presented here is in order. In the present study only phononic band gaps are studied as pass and stop bands are related to tuning in an acoustic medium. Phenomena as Bragg diffraction or Umklapp processes are not considered. Acoustic metamaterials are understood to be those with resonant units whose resonance frequency is well below the wavelength established by Bragg's criterion and possess such features as negative group velocity. While Bragg's diffraction and associated phenomena are interesting in nature, the study of such cases are deemed irrelevant and fall beyond the scope of the present work.

Acknowledgements

The authors are grateful for the financial support provided by the US Office of Naval Research (ONR) under grant number N00014-07-1-0496. One of the authors (YY) is grateful for the partial financial support he received from ORSAS of the UK. This work is declared a work of the US Government and is not subject to copyright protection in the United States.

References:

[1] A.D. Boardman, O. Hess, R.C. Mitchell-Thomas, Y.G. Rapoport, L. Velasco, Temporal solitons in magnetooptic and metamaterial waveguides, Photonics and Nanostructures - Fundamentals and Applications, 8 (2010) 228-243.
[2] J.B. Pendry, Negative refraction makes a perfect lens, Physical Review Letters, 85 (2000) 3966-3969.
[3] D.R. Smith, Metamaterials and negative refractive index, Science, 305 (2004) 788.
[4] K.B. Alici, A.E. Serebryannikov, E. Ozbay, Photonic magnetic metamaterial basics, Photonics and Nanostructures - Fundamentals and Applications, 9 (2011) 15-21.
[5] A. Baz, The structure of an active acoustic metamaterial with tunable effective density, New journal of physics, 11 (2009) 123010.
[6] H.H. Huang, Wave attenuation mechanism in an acoustic metamaterial with negative effective mass density, New journal of physics, 11 (2009) 013003.
[7] G.L. Huang, Band gaps in a multiresonator acoustic metamaterial, Journal of vibration and acoustics, 132 (2010) 31003.
[8] Z. Liu, Analytic model of phononic crystals with local resonances, Physical review. B, Condensed matter, 71 (2005) 014103.
[9] Z. Liu, X. Zhang, Y. Mao, Y.Y. Zhu, Z. Yang, C.T. Chan, P. Sheng, Locally resonant sonic materials, Science, 289 (2000) 1734-1736.
[10] X. Zhang, Z. Liu, Negative refraction of acoustic waves in two-dimensional phononic crystals, Applied physics letters, 85 (2004) 341-343.
[11] J. Li, C.T. Chan, Double-negative acoustic metamaterial, Physical Review E, 70 (2004) 055602.
[12] W.J. Padilla, Negative refractive index metamaterials, Materials today, 9 (2006) 28.
[13] C.G. Poulton, Eigenvalue problems for doubly periodic elastic structures and phononic band gaps, Proceedings - Royal Society. Biological sciences, 456 (2000) 2543.
[14] M.S. Kushwaha, P. Halevi, L. Dobrzynski, B. Djafari-Rouhani, Acoustic band structure of periodic elastic composites, Physical Review Letters, 71 (1993) 2022-2025.
[15] V.V. Zalipaev, A.B. Movchan, I.S. Jones, Two-parameter asymptotic approximations in the analysis of a thin solid fixed on a small part of its boundary, The Quarterly Journal of Mechanics and Applied Mathematics, 60 (2007) 457-471.
[16] P.G. Martinsson, Vibrations of lattice structures and phononic band gaps, The Quarterly Journal of Mechanics and Applied Mathematics, 56 (2003) 45.
[17] G. Wang, Lumped-mass method for the study of band structure in two-dimensional phononic crystals, Physical review. B, Condensed matter, 69 (2004) 184302.
[18] V.G. Veselago, The electrodynamics of substances with simultaneously negative values of ε and μ, Physics-Uspekhi, 10 (1968) 509-514.
[19] G. Kron, Tensor analysis of networks, J Wiley & Sons, New York, 1939.
[20] H. Huang, C. Sun, Wave attenuation mechanism in an acoustic metamaterial with negative effective mass density, New journal of physics, 11 (2009) 013003.
[21] C. Kittel, Elementary Solid State Physics: A Short Course, Wiley, New York, 1962.
[22] L. Brillouin, Wave Propagation in Periodic Structures, McGraw Hill Co., New York, 1946.

[23] J.W. A. Srikantha Phani, and N. A. Fleck, Wave propagation in two-dimensional periodic lattices, J. Acoust. Soc. Am., 119 (2006) 1995-2005.
[24] Y. Yang, A.S. Fallah, L.A. Louca, Frequency analysis of a heterogeneous perforated panel using a super-element formulation, Journal of Sound and Vibration, 327 (2009) 26-40.

Appendix A:

a. Derivation of pass and stop bands for the 2D anisotropic phononic metamaterial:

This section of appendix A presents and implements the algorithm used to derive the band diagram for the 2D anisotropic metamaterial under consideration. As a first step the harmonic plane wave solution of equations (A.1)-(A.3) is substituted into the equations of motion (equations (5)-(9)). For the horizontal displacement component, for instance, the displacement, velocity and acceleration are shown by equations (A.4)-(A.6). The substitution in the first equation of motion (A.7) i.e. the horizontal motion of the internal mass results in equation (A.8). Other equations concerning vertical motion of the internal mass and horizontal and vertical motions of the outer mass are obtained in a similar fashion. These equations are generally very lengthy and need to be put into the matrix form. When the periodic boundary conditions are applied these equations are reduced to (A.9) where the reduced mass and stiffness matrices are introduced in (A.10) and (A.11).

The harmonic plane wave solution:

$$u = A_u e^{i(k_x x + k_y y - \omega t + \theta)} \quad (A.1)$$

$$u = A_u e^{i\theta} e^{i(k_x x + k_y y - \omega t)} \quad (A.2)$$

$$u = S_u e^{i(k_x x + k_y y - \omega t)} \quad (A.3).$$

Horizontal displacement/velocity/acceleration for the phonon in row p and column q:

$$u^{p,q} = S_u^{p,q} e^{i(k_x qa + k_y qb - \omega t)} \quad (A.4)$$

$$\dot{u}^{p,q} = -i\omega S_u^{p,q} e^{i(k_x qa + k_y qb - \omega t)} \quad (A.5)$$

$$\ddot{u}^{p,q} = -\omega^2 S_u^{p,q} e^{i(k_x qa + k_y qb - \omega t)} \quad (A.6).$$

The first equation of motion:

$$m_i^{p,q} \ddot{u}_i^{p,q} = k_{iu}\left(u_e^{p,q} - u_i^{p,q}\right) \quad (A.7).$$

Recast equation (A.7) using the harmonic plane wave solution of equations (A.4)-(A.6):

$$S_{iu}^{p,q}k_{iu} - S_{eu}^{p,q}k_{iu} - m_i^{p,q}\omega^2 S_{iu}^{p,q} = 0 \qquad \text{(A. 8)}$$

$$\boldsymbol{K} - \omega^2\boldsymbol{M} = \boldsymbol{0} \qquad \text{(A. 9)}$$

$$\boldsymbol{M} = \begin{bmatrix} m_i & 0 & 0 & 0 \\ 0 & m_i & 0 & 0 \\ 0 & 0 & m_e & 0 \\ 0 & 0 & 0 & m_e \end{bmatrix} \qquad \text{(A. 10)}$$

$$\boldsymbol{K} = \begin{bmatrix} k_{11} & 0 & -k_{11} & 0 \\ 0 & k_{22} & 0 & -k_{22} \\ -k_{11} & 0 & k_{33} & k_{34} \\ 0 & -k_{22} & k_{34} & k_{44} \end{bmatrix} \qquad \text{(A. 11).}$$

The entries being defined as:

$$k_{11} = k_{iu}$$
$$k_{22} = k_{iv}$$
$$k_{33} = -(k_i E_1 cos^2\theta + k_{eu}E_3 - k_{iu})$$
$$k_{34} = -sin\theta\ cos\theta k_i E_2,$$

And

$$k_{44} = -(k_i E_1 sin^2\theta + k_{ev}E_4 - k_{iv}),$$

Where

$$E_1 = e^{i(-k_x a - k_y b)} + e^{i(k_x a - k_y b)} + e^{i(-k_x a + k_y b)} + e^{i(k_x a + k_y b)} - 4$$
$$E_2 = e^{i(-k_x a - k_y b)} - e^{i(k_x a - k_y b)} - e^{i(-k_x a + k_y b)} + e^{i(k_x a + k_y b)}$$
$$E_3 = e^{i(-k_x a)} + e^{i(k_x a)} - 2$$
$$E_3 = e^{i(-k_y b)} + e^{i(k_y b)} - 2,$$

Once the problem has been formulated and the ***k***-space locus established the following procedure will be followed to extract the band diagram:

Initialisation:

1. Define the irreducible Brillouin Zone relevant to the system being modelled. In all cases where $\gamma \neq 1$this is a rectangle in the ***k***-space locus. In the case of $\gamma = 1$it is a right triangle.
2. Set up as constants as many parameters as the rank of the dimensionality matrix (e.g. $\beta, b, k_{eu}, k_i, m_e$).
3. Set up values defining the current plot (α, γ).

4. Calculate the remaining parameters using the current values of α &γ i.e. a, m_i and spring stiffnesses.
5. Set up the mass matrix.

Main body calculations:

1. Loop pointing to each of the four sides (or three sides in the case of $\gamma = 1$) of the BZ in turn.
2. Loop defining discrete points on the current side of BZ.
3. Calculate the components of the wave vector for the current point on the BZ. The current values of $k_x$and $k_y$represent the abscissa for the dispersion plot through the arc length parameter *s*.
4. Set up the modified stiffness matrix for the current $k_x$and k_y.
5. Calculate the eigenvalues of the dynamic matrix $\boldsymbol{D} = \boldsymbol{K} - \boldsymbol{M}\omega^2$and solve equation (18).
6. Sort the eigenvalues ω^2 in the ascending order. The ω values are the ordinates of the dispersion plot. They can be used as absolute values or non-dimensionalised using a parameter of the same dimension.
7. Store the values of the ordered triple (k_x, k_y, ω) or the ordered pair $(s, \omega)$to be plotted.

The procedure above was programmed into a Python script which produced the band structure. As a benchmark problem a 1D case from the literature was adopted and the results of the method were corroborated with those of the literature obtained using a different method. The following section encompasses the results.

b. An example of correlation of the formulation with a 1D phononic metamaterial (Huang and Sun [20])

A Python script was used to generate the dispersion plots presented here, in order to validate this script we chose to replicate the 1D infinite latticed metamaterial and corresponding dispersion plot that Huang and Sun [20] give in figure (A.2). The lattice is indicated in figure (A.1) some comments on how the 2D Python script is used to model this 1D lattice are given below:

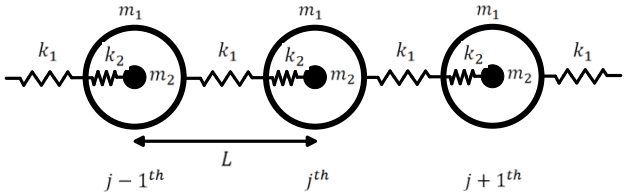

Figure A1: the infinite 1D metamaterial (based on Huang and Sun [20])

- The stiffness values used in the script for k_{iv}, k_{ev} and k_i are much smaller than the values for k_{eu} and k_{iu}. Thus the modal frequencies for the two vertical modes are much lower than the frequencies for the horizontal modes and therefore have little influence on the band gap shown in the dispersion plot. On close inspection of the dispersion plot in figure (A.2) it can be seen that the two curves for the vertical modes are shown as a green line on the horizontal axis.
- The vertical component of the wave vector, k_y, remains zero at all times. Referring to figure 4 the relevant portions of the irreducible Brillouin zone are Γ-P & Q-R, i.e. $-\pi/a \leq k_x \leq \pi/a$ and $k_y = 0$.
- Following the normalisation method of Huang and Sun [20] the dispersion plot in figure (A.2) shows the frequency normalized with respect to the local resonant frequency of the internal mass, $\omega_0 = \sqrt{\frac{k_{iu}}{m_i}}$.

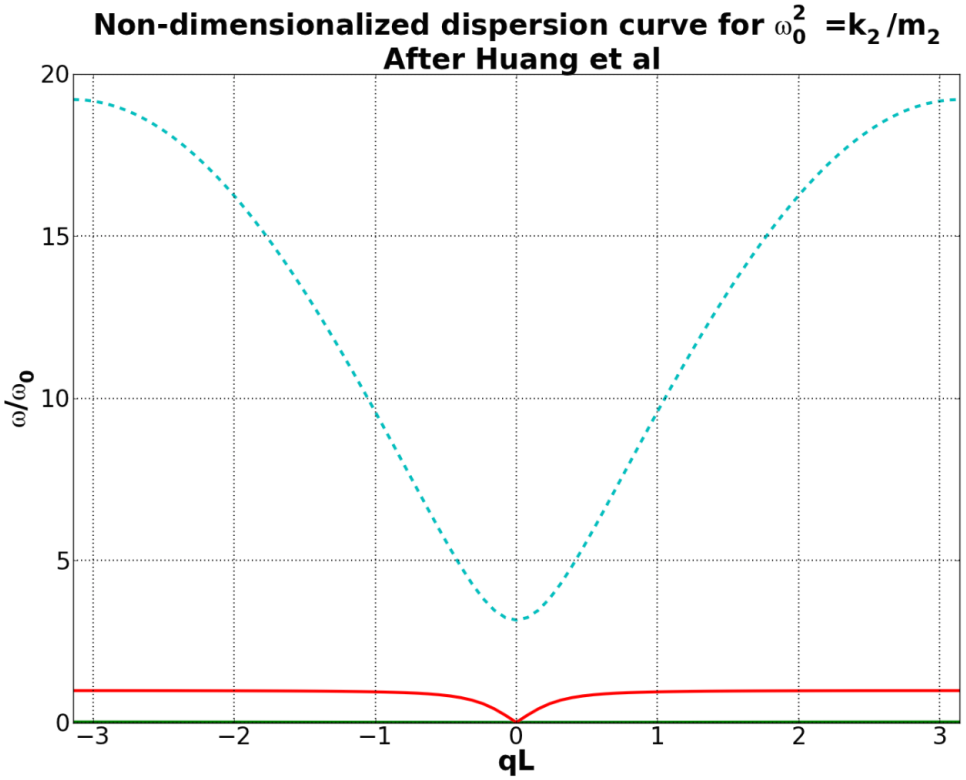

Figure A2: Validation of the dispersion plot matching that given by Huang and Sun [20]

Appendix B:

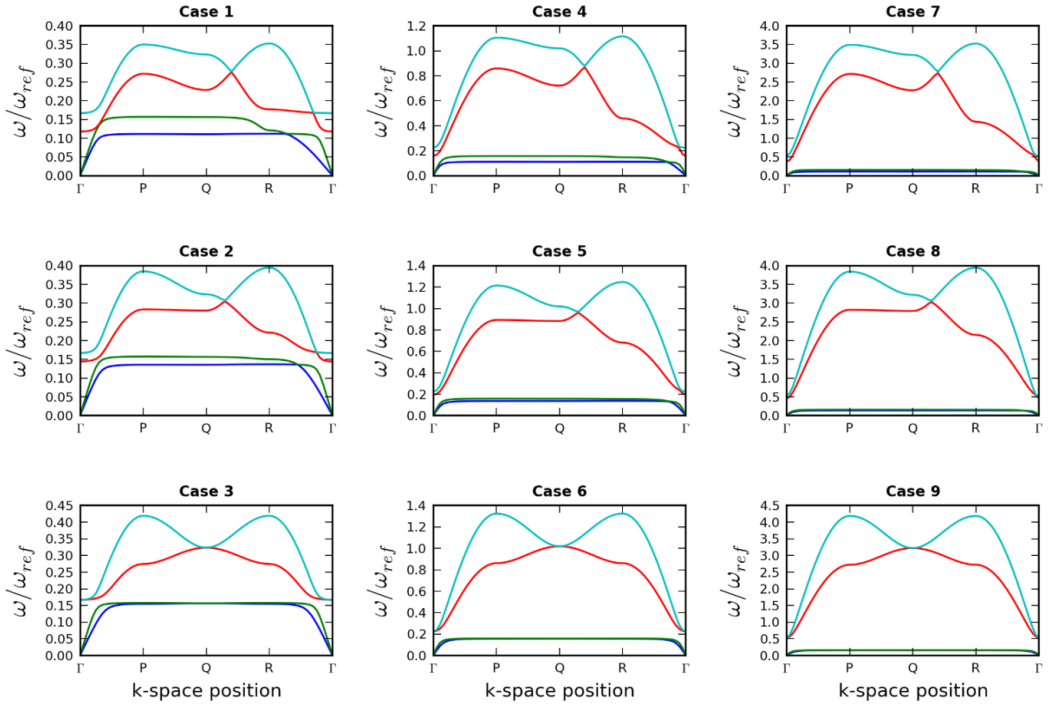

(a)

Figure B1: Comparison of frequency pass and stop bands for (a) $\beta = 0.1$, (b) $\beta = 1.0$ and (c) $\beta = 10$

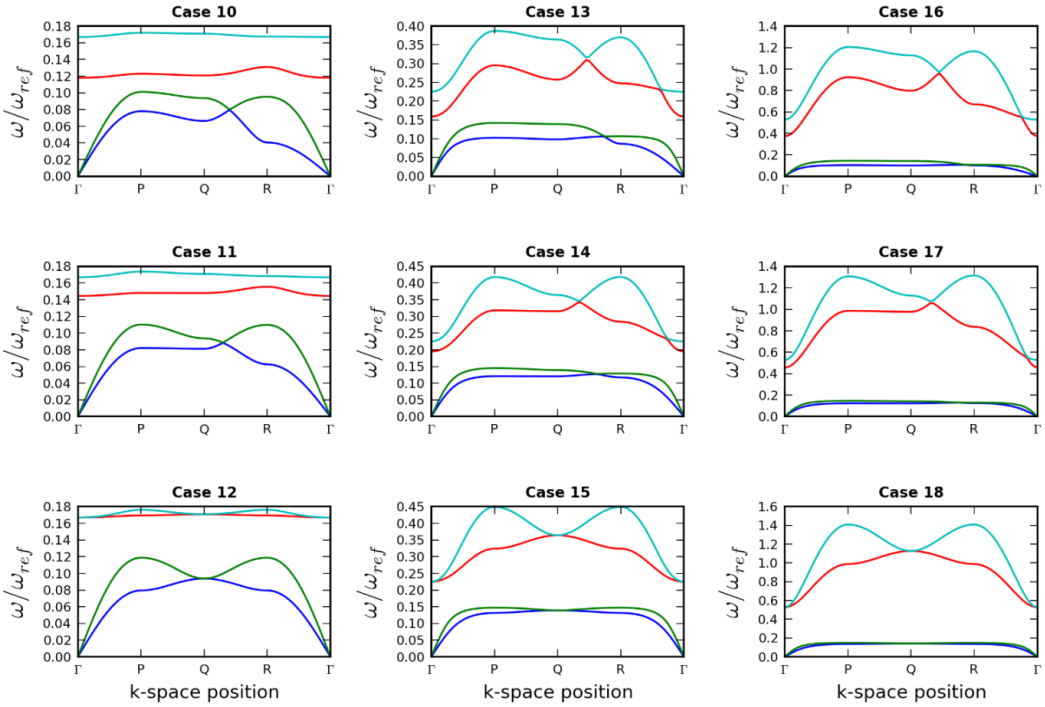

Figure B1 (b)

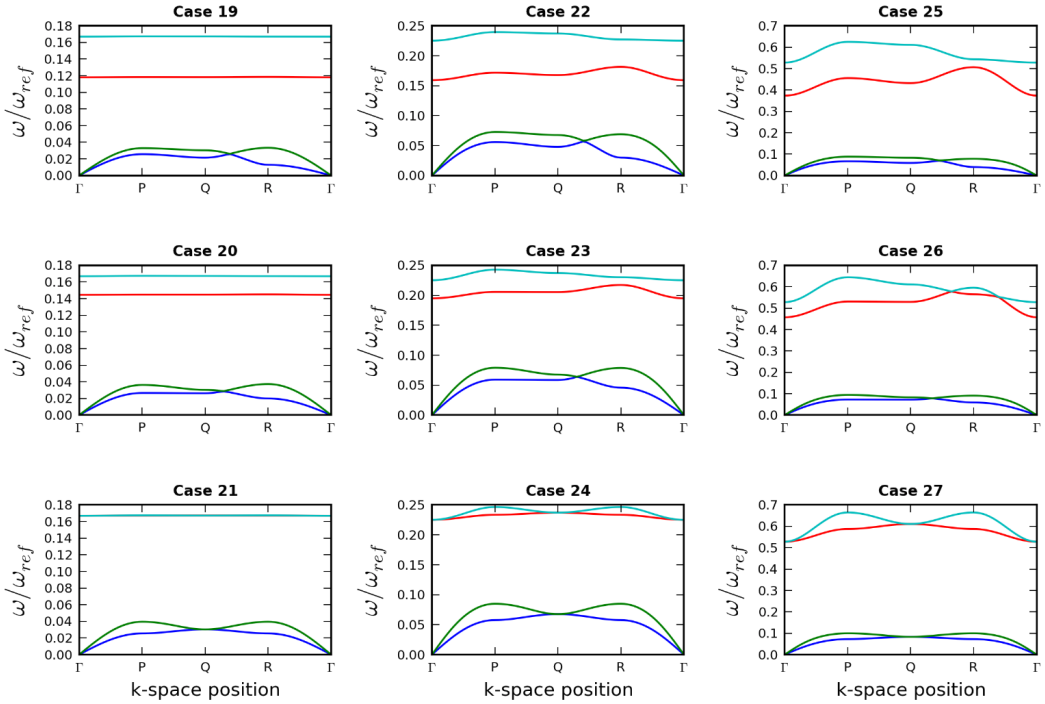

Figure B1(c)